37th AIAA Thermophysics Conference, Portland, OR, 2004.
AIAA-2004-2455

Uncertainty and Sensitivity Analysis of Thermochemical Modeling for Titan Atmospheric Entry

Deepak Bose*, Michael Wright†, and Tahir Gökçen‡
NASA Ames Research Center
Moffett Field, CA 94035

Abstract

A Monte Carlo uncertainty and sensitivity analysis technique is presented to i) identify the major sources of uncertainty in the thermochemical models used for aerothermal analysis, and ii) track the propagation of these uncertainties through the system into the predicted quantities of interest, such as the vehicle heating, shock layer properties, etc. The technique is applied to the aerothermal analysis of Titan aerocapture, where CN shock layer radiation is the dominant source of vehicle heating. Several hundred model input parameters, including reaction rate constants, vibration-chemistry coupling parameters, vibrational relaxation times, and transport properties, are independently sampled over their range of uncertainties, and the vehicle heating is determined probabilistically. A massively parallel, axisymmetric CFD (Data-Parallel Line Relaxation) code was used to make the several thousand runs needed to statistically describe the variability in the heating predictions. It is found that major contributions to the uncertainty in the predicted heating originates from the uncertainties in the rates of N_2 dissociation by H atom impact, and some atomic exchange reactions: $N_2+H \rightarrow NH+N$ and $N_2+C \rightarrow CN+N$.

I. Introduction

An aerocapture mission to Saturn's largest moon, Titan, is being considered by NASA's In-Space Propulsion program.[1] Aerocapture is a means of aerodynamically decelerating a vehicle in a single pass through the atmosphere and capture into orbit upon its arrival at a destination planet. Due to minimal use of on-board propulsion to attain the target orbit, this approach offers propellant mass savings at the expense of the mass of the Thermal Protection System (TPS) needed to protect the vehicle from aerodynamic heating. To successfully make the trade between the orbital insertion propellant weight versus the TPS weight, an aerothermal analysis of the vehicle during the aerocapture maneuver with a specified level of confidence is essential.

Prior aerothermal studies[2-5] using a baseline vehicle geometry and a set of bounding entry trajectories (entry speed ≥ 6 km/s) have shown that the fore body heating of the vehicle will be dominated by shock layer radiation. Furthermore, it has been determined that below an entry speed of about 8 km/s, 99% of the radiation intensity is due to spontaneous de-excitation of CN molecules from higher electronic states, chief among them are the violet ($B^2\Sigma^+ \rightarrow X^2\Sigma^+$) and the red ($A^2\Pi \rightarrow X^2\Sigma^+$) bands. The CN molecules are formed via shock heated dissociation and exchange of nitrogen and methane (and intermediate species) in the Titan atmosphere. The aerothermal simulations were performed using CFD and nonequilibrium radiation codes at NASA Ames and Langley Research Centers. Over the years these codes have been tested against each other and against a variety of experimental data from wind tunnel tests and flight tests.[6-11] Based on these test analyses and comparisons, it can be clearly demonstrated that the heating predictions made by these tools are highly sensitive to the physical, chemical

* ELORET Corporation, Member AIAA, Email: dbose@arc.nasa.gov
† Senior Member AIAA
‡ ELORET Corporation

and numerical models employed and the selection of the model parameters. Consequently, the uncertainties in the heating predictions are a result of a combined effect of the uncertainties in all the models and parameters used in the analysis. Therefore, in order to place confidence levels on the heating predictions, chief sources of uncertainty must be identified and quantified. The propagation of these uncertainties through the model must then be tracked to make probabilistic estimates of the vehicle heating; namely the most likely heating value and a probability distribution characterizing the variability of the prediction. This probabilistic determination can be integrated further with the mission risk analysis process. The results of the uncertainty analysis also help scientists and engineers focus their efforts only on reducing the largest sources of uncertainty, resulting is a greater incremental benefit for the resources spent on research.

Sources of uncertainty in the thermochemical models used in aerothermal analysis, like other physical models, may be classified into three categories- structural uncertainty, parametric uncertainty, and stochastic variability.

1. *Structural uncertainty*

All mathematical models use a set of simplifying assumptions to represent the physical phenomena being studied. These simplifications, mostly incorporated for the purposes of tractability, can be significant sources of uncertainties. Examples of these uncertainties in thermochemical models include limitation inherent in the continuum formulation of the governing equations, representation of their boundary conditions, limitations of their discretized representation, assumption of a specific energy distribution function, use of a simplified radiative transport, and perhaps impact of other unknown mechanisms. These uncertainties are usually difficult to quantify and one has to rely on expert judgment and past experiences of successful (or unsuccessful) validation against similar experiments. Obviously, structural uncertainty is larger in a regime where the models have not been validated. In this work we will not deal with this type of uncertainty, as it requires in-depth evaluation of the foundations of the model, which is beyond the scope of the current work.

2. *Parametric uncertainty*

This type of uncertainty arises from the uncertainties in the model parameter estimates. Examples of these parameters are chemical reaction rates, thermal relaxation rates, vibration-dissociation coupling parameters, transport properties, wall catalycity, freestream conditions, emission and absorption rates, etc. For aerothermal analysis a large set of parameters is needed, while only a handful of them have been experimentally measured or theoretically calculated (using *ab initio* techniques, for example). A majority of these parameters are estimated either by indirect or purely empirical techniques. The purpose of this work is to identify the chief sources of parametric uncertainties in the aerothermal analysis of Titan aerocapture. These parameters are ranked not only based on the uncertainty of their values, but also on the sensitivity of the output quantity of interest to these parameters. For the radiative heat flux we expect the parametric uncertainty to be a significant component of the total uncertainty. Titan shock layer radiation is strongly dependent on the density of CN and the temperatures in the shock layer, which mostly suffer from parametric uncertainties due to lack of knowledge of reaction rate parameters, relaxation rates, transport properties etc. The determination of CN excited states from the ground state CN density and temperatures may, however, suffer from significant structural uncertainty due to a Boltzmann assumption. This type of uncertainty will be addressed in a future article by evaluating the validity of the Boltzmann assumption via comparisons with the shock tube radiation measurements.

3. *Stochastic variability*

This type of uncertainty arises due to natural fluctuations that exist in the physical environment. It is also known as irreducible uncertainty, which can be characterized better with additional experimentation, but not reduced. Examples in aerothermal analysis include fluctuations in atmospheric conditions, random variations and adjustments in the trajectory, etc. The worst case scenario is often considered for design purposes. Since this paper deals with uncertainties in thermochemical models, this type of uncertainty is not considered.

This article describes the Monte Carlo uncertainty analysis used for non-linear systems. The technique is applied to the Titan aerothermal analysis with a goal of predicting heating of the vehicle due to CN radiation. The assessment of the uncertainty will be discussed for some of the important model parameters. Finally the results of the Monte Carlo analysis will be discussed and interpreted.

II. Flowfield and Radiation Computations

.

The maximum radiative heating from aerothermal analyses[2-5] was predicted to occur at t = 253 s on the minimum atmosphere lift-up trajectory, with freestream conditions given by 95% N_2, 5% CH_4 by mole, $\rho_\infty = 1.49 \times 10^{-4}$ kg/m^3, $V_\infty = 5.76$ km/s, and $T_\infty = 152.7$ K. All analysis in the present work will be centered on this peak heating point (see Ref. 3 for more information). The Monte Carlo methodology employed for the present analysis requires the computation of a large number of cases to ensure statistically meaningful results. Since our primary interest is the radiative heating at the stagnation streamline, we simplify the geometry to a sphere with a diameter of 2 m with a similar stagnation region.

The flowfield computations are performed using the computational fluid dynamics (CFD) code DPLR.[12] DPLR is a parallel multiblock finite-volume code that solves the Navier-Stokes equations including finite-rate chemistry and the effects of thermal nonequilibrium. DPLR, along with the code LAURA[13], were the primary tools used to develop the aeroheating predictions in the systems analysis study[2-5] In addition to the conservation equations for mass and momentum, two energy equations are solved; a total energy equation and a combined vibro-electronic energy equation. In this formulation it is assumed that the vibrational and electronic modes of the gas are in equilibrium with each other, but not with the translational-rotational component. The energy exchange between the translational-rotational and vibrational-electronic modes is modeled using a Landau-Teller formulation, where relaxation times are obtained from Millikan and White,[14] assuming simple harmonic oscillators. One vibrational temperature is used for all polyatomic species. Characteristic vibrational temperatures for the simple harmonic oscillator approximation are taken from Gurvich et al.[15] A 13-species (CH_4, CH_3, CH_2, HCN, N_2, C_2, H_2, CH, NH, CN, N, C, H) 26-reaction finite-rate chemistry model is used in this paper. The chemical source terms are modeled using rates collected for the Titan entry problem by Gokcen.[16] Viscosity and thermal conductivity are modeled using the species expressions and mixing rules presented by Gupta et al.[17] Collision integrals are taken from Park et al.[18] for most binary interactions. Collision integrals for all other interactions were computed using a modified Lennard-Jones potential[18] for the neutral-neutral interactions and a polarization potential for the ion-neutral interactions. The self-consistent effective binary diffusion (SCEBD) method[19] is used to model mass diffusion fluxes. Radiation-flowfield coupling was modeled following the method detailed in Ref. 5, using curve fits of CN (violet and red) intensities from the line-by-line radiation code NEQAIR[20] and assuming that the flowfield was optically thin to the emitted shock layer radiation. The stagnation point radiative heating is computed using a tangent slab approximation. For further details on the flowfield and radiation computations, the reader is referred to Ref. 5.

Since the majority of the radiation is generated in the inviscid portion of the shock layer, the computed stagnation point radiative heating is weakly sensitive to the level of grid resolution since the boundary layer resolution is not needed. A grid density of 20x40 points was determined to be sufficient. On this baseline grid a fully converged solution was produced in about 50-60 seconds on 5 CPUs of an Intel Xeon cluster. Therefore a full sample of 6000 cases takes only slightly more than four days.

III. Sensitivity and Uncertainty Analysis

A. Local Analysis

For linear systems and systems where the uncertainties at play are small, a linear sensitivity and uncertainty analysis may be used. In such an analysis, sensitivity coefficients, $\partial y_i/\partial x_j$, that determine the change in the output parameter, y_i, caused by an infinitesimal change in the input parameter x_j, from its reference or most probable value are evaluated. The sensitivity coefficients can be computed numerically by recording the changes in the output, as each input parameter is varied by infinitesimally small amount, while all other parameters are held constant. Alternatively, sensitivity coefficients may be obtained by differentiating the governing equations with respect to all the input parameters and solving the resulting system of equations with the sensitivity coefficients as unknowns. Once the sensitivity coefficients are determined, the uncertainty in the output parameter is described by the law of propagation of errors,

$$\sigma^2(y_i) = \sum_k \left(\frac{\partial y_i}{\partial x_k} \right)^2 \sigma^2(x_k) \tag{1}$$

where $\sigma^2(y_i)$ is the variance (uncertainty) in the value of the output y_i and $\sigma^2(x_k)$ is the corresponding variance in the in the input parameter x_k. The input parameter (e.g. reaction rates, transport properties, etc.) uncertainties are determined either from the original source in the literature or from using expert judgment by combining several sources of data. Often, there is no experimental or theoretical evaluation of the input parameter, which requires the use of expert judgment in estimating not only the value of the parameter but also the accompanying uncertainty. Although computationally efficient, the linear analysis outlined here is a local analysis, *i.e.* the analysis yields sensitivity coefficients only in the neighborhood of the baseline values in parameter space. However, in aerothermal analysis, the variability in input parameters can be quite large. The sensitivity coefficients may not only vary substantially in the zone of variability in the parameter space, but may also interfere with the sensitivities of other input parameters. Therefore, a non-linear global uncertainty analysis is necessary.

B. Global Analysis

Apart from the ability to treat large variabilities in the input and output parameters, a global model allows simultaneous variation of input parameters in order to account for uncertainty and sensitivity interference effects. In the present work, a Monte Carlo technique, which is well suited for this purpose, is used. In this technique the input parameters are varied independently using a probability distribution function. We choose a Gaussian function to describe the uncertainty of each input parameter; the maximum of the function is set at the recommended value, while the width of the curve represents the uncertainty in the parameter. We assume that the probability distribution functions are symmetric about the recommended parameter values and that the uncertainties of all input parameters are uncorrelated. Note that these restrictions are not imposed by the Monte Carlo technique. Rather, they are necessitated by the lack of detailed information on input uncertainties. The steps involved in the Monte Carlo technique are as follows. For details the reader is referred to Ref. 21.

1) Uncertainties are assigned in terms of 95% confidence limits based on literature review or author's judgment. Gaussian probability functions are built based on these uncertainties.
2) Random numbers are used to sample input parameter values based on their probability distribution function.
3) A DPLR+NEQAIR run is made with the selected input parameters and the output values of interest (radiative heat flux) are collected.
4) Steps (2) and (3) are repeated with different random numbers until a statistically significant sample describing the input and output probability distributions are obtained. In this work we made about 6000 runs of DPLR on an axisymmetric body, which is considered enough to identify the large sources of uncertainties.
5) Correlation coefficients are obtained for each input-output pair.
6) Uncertainty contributions to the output are identified and ranked.

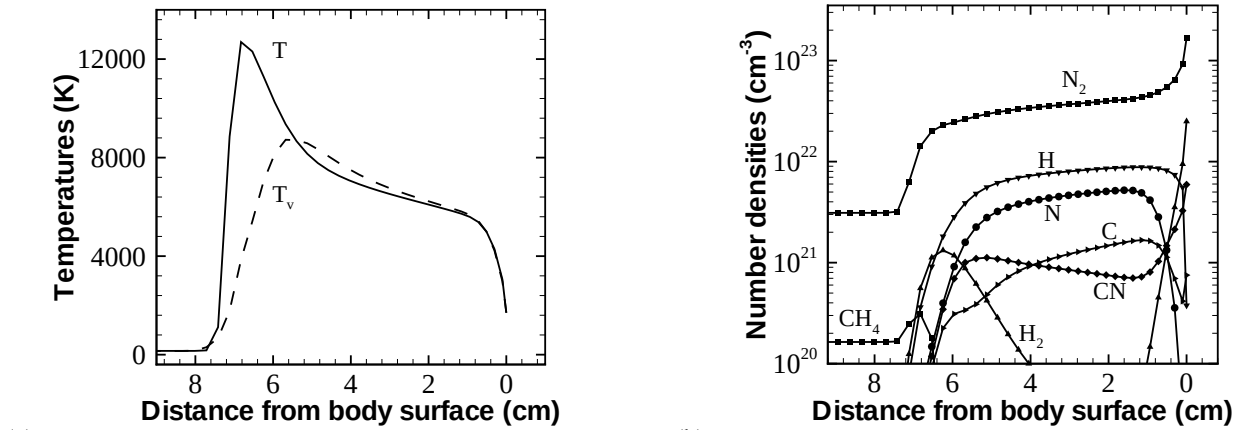

Fig. 1. Extracted profiles of flowfield quantities along stagnation streamline from axisymmetric computations. (a) Translational-rotational, T, and vibrational temperature, T_v, and (b) selected species number densities. This is also the line of sight for radiation flux calculation at the stagnation point.

Table 1. The reduced reaction mechanism for Titan shock layer, obtained from Ref. 16. The paper details the Arrhenius parameters of the rate constants and lists their sources. The uncertainties in the rate constants [$\log_{10} k_r$] are presented in the form of 95% confidence limits, equal to ±2σ for a Gaussian probability distribution. The references for the uncertainties are shown in the brackets. The numbers marked with [T] are estimated in this work and are discussed in the text.

	Dissociation reactions $k_f=A_rT^{br}\exp(-C_r/T)$	A_r(cc/mol-s)	b_r	C_r (K)	95% conf. limit [Ref.]
1	$N_2 + M \Leftrightarrow 2N+M$	7.00×10^{21}	-1.60	113200	See Table 2
	M=N,C,H	3.00×10^{22}	-1.60	113200	
2	$CH_4 + M \Leftrightarrow CH_3 + H + M$	4.70×10^{47}	-8.20	59200	±0.30[22]
3	$CH_3 + M \Leftrightarrow CH_2 + H + M$	1.02×10^{16}	0.00	45600	±0.35[22]
4	$CH_3 + M \Leftrightarrow CH + H_2 + M$	5.00×10^{15}	0.00	42800	±0.30[23]
5	$CH_2 + M \Leftrightarrow CH + H + M$	4.00×10^{15}	0.00	41800	±0.30[23]
6	$CH_2 + M \Leftrightarrow C + H_2 + M$	1.30×10^{14}	0.00	29700	±0.30[23]
7	$CH + M \Leftrightarrow C + H + M$	1.90×10^{14}	0.00	33700	±0.30[23]
8	$C_2 + M \Leftrightarrow 2C + M$	1.50×10^{16}	0.00	71600	±0.30[24]
9	$H_2 + M \Leftrightarrow 2H + M$	2.23×10^{14}	0.00	48350	±0.30[22,25]
10	$CN + M \Leftrightarrow C + N + M$	2.53×10^{14}	0.00	71000	±0.30[26,27]
11	$NH + M \Leftrightarrow N + H + M$	1.80×10^{14}	0.00	37600	±0.30[28]
12	$HCN + M \Leftrightarrow CN + H + M$	3.57×10^{26}	-2.60	62845	±0.30[29]
	Exchange reactions				
13	$CH_3 + H \Leftrightarrow CH_2 + H_2$	6.03×10^{13}	0.00	7600	±1.00[25]
14	$CH_2 + N_2 \Leftrightarrow HCN + NH$	4.82×10^{12}	0.00	18000	±1.00[28]
15	$CH_2 + N \Leftrightarrow HCN + H$	5.00×10^{13}	0.00	0	±1.00[30]
16	$CH_2 + H \Leftrightarrow CH + H_2$	6.03×10^{12}	0.00	-900	±0.87[25,28]
17	$CH + N_2 \Leftrightarrow HCN + N$	4.40×10^{12}	0.00	11060	±0.35[30]
18	$CH + C \Leftrightarrow C_2 + H$	2.00×10^{14}	0.00	0	±1.00[23]
19	$C_2 + N_2 \Leftrightarrow 2CN$	1.50×10^{13}	0.00	21000	±0.30[31]
20	$CN + H_2 \Leftrightarrow HCN + H$	2.95×10^{5}	0.00	1130	±0.60[32]
21	$CN + C \Leftrightarrow C_2 + N$	5.00×10^{13}	0.00	13000	±0.54[18]
22	$N + H_2 \Leftrightarrow NH + H$	1.60×10^{14}	0.00	12650	±0.30[33]
23	$C + N_2 \Leftrightarrow CN + N$	5.24×10^{13}	0.00	22600	±0.50[T]
24	$C + H_2 \Leftrightarrow CH + H$	4.00×10^{14}	0.00	11700	±0.30[34]
25	$H + N_2 \Leftrightarrow NH + N$	3.00×10^{12}	0.50	71400	±0.50[T]
26	$CH_4 + H \Leftrightarrow CH_3 + H_2$	1.32×10^{4}	3.00	4045	±0.30[22,25]

IV. Estimated Input Parameter Uncertainties

Estimation of uncertainties associated with the input parameters is often a subjective issue on which experts may express differing opinions. However, in order to carry out any probabilistic analysis, where human judgment is involved, a good practice is to consider and incorporate a variety of such expert opinions. Statistically, uncertainty is defined as the standard error of the mean from a sample of measurements. However, since multiple measurements are rare for the input parameters that are being considered in this work, the uncertainties are mostly estimated or, in some cases, are taken from the literature. We consider four different categories of parameters that are used by DPLR; reaction rate coefficients, vibration-chemistry coupling parameters, vibration-translational relaxation rates, and transport properties (diffusion coefficients, viscosity, and thermal conductivity). The input parameters used in

NEQAIR such as the radiative transition probabilities are not treated in the uncertainty analysis. The collisional excitation and de-excitation rates are not used in the current approach since a Boltzmann distribution of the CN excited state population is assumed. This assumption will be relaxed in future.

Table 2. Estimated uncertainties in the rate [$\log_{10} k_r$] of dissociation of N_2 with different collision partners. See text for references and discussion.

Coll. Partner	N_2	CH_4	CH_3	CH_2	CH	CH	C_2
95% conf. limit	±0.25	±0.50	±0.50	±0.50	±0.50	±0.50	±0.50
Coll. Partner	H_2	CN	NH	HCN	N	C	H
95% conf. limit	±0.50	±0.50	±0.50	±0.50	±0.60	±0.60	±0.75

A. Reaction Rate Constants

Our 13 species system, as mentioned before, has no electrons or ions. Under the conditions being considered, the charged species densities were determined by the previous aerothermal studies[2-5] to be too low to affect the flow properties. A detailed set of reactions for N_2-CH_4 system relevant for shock layers will be discussed in a companion paper.[16] In this work, however, we will only consider a systematically reduced set of 26 reactions as recommended by Gokcen.[16] The reactions are listed in Table 1 with the recommended rates. This mechanism is similar to the one used by Nelson *et al.*[35] with a few additional reactions. The rate parameters are however different.

Since the rates of most of these reactions are either undetermined or are measured at temperature below 4000 K, the uncertainties in the rates can be quite large. It is therefore appropriate to consider the rate constant uncertainties on a logarithmic scale. The Gaussian probability distribution of a sampled rate constant k_r can then be written as

$$P(k_r) \propto \exp\left[-\frac{1}{2}\left(\frac{\log_{10} k_r / k_r^0}{\sigma}\right)^2\right], \tag{2}$$

where $\pm 2\sigma$ defines the 95% confidence limits symmetrically bounding the recommended rate constant, k_r^0. $P(k_r)$ is the probability that the actual rate constant of reaction r is k_r. It also implies that the actual rate constant lies within $\log_{10} k_r^0 \pm 2\sigma$ with 95% probability. The sampling of a rate constant over the distribution function is obtained by varying only the pre-exponential factor, A_r, of the Arrhenius rate expression: $k_r = A_r T^{br} \exp(-C_r/T)$. b_r and C_r are considered fixed. In order to vary b_r, temperature dependent uncertainty information is needed, which is almost never available.

1. *Dissociation Reactions*

Since the Titan atmosphere is composed of about 97% N_2 (with some variability), the rate of dissociation of N_2 is likely to be an important source of uncertainty. This was recognized earlier by Olejniczak *et al.*[3] who demonstrated the high sensitivity of radiative heating to the rate of N_2 dissociation. In this work we seek to further distinguish the sensitivities (and uncertainties) caused by dissociation processes with individual collision partners. The best available rates for N_2 dissociation with N_2, N and Ar as collision partners are described by Park.[36] These rates were obtained by re-interpreting three different sets of shock tube data of density profiles downstream of the shock. Park used his two temperature model ($\sqrt{TT_v}$) to account for the vibration dissociation coupling and found that the re-interpreted rate constants from these sources are described very well by his recommended expression (see Table 1). He however cautioned that the rates are somewhat uncertain due to the negative feedback between the vibrational relaxation and dissociation. As dissociation proceeds, it preferentially depletes the high vibrational energy oscillators, thereby reducing the vibrational temperature and resulting in a slower dissociation. Therefore, since the extent of dissociation is controlled by additional uncertainties caused by preferential removal of vibrational energy etc, the re-interpreted rates are, consequently, somewhat uncertain. Park recommended a factor of 1.5

uncertainty for the rate of $N_2+N_2 \rightarrow 2N+N_2$ reaction. Since this reaction is critical in the Titan shock layer, we conservatively choose as 95% confidence limit of a factor of 3 ($4\sigma = 0.5$ in the $\log_{10}$ scale). The rates of dissociation of N_2 with other molecular species as collision partners are unlikely to be important since the next most abundant molecular species in the shock layer has about three orders of magnitude lower density than that of N_2. Due to the lack of available data, we assume their rates to be the same as the rate of $N_2+N_2 \rightarrow 2N+N_2$ reaction, although with an increased uncertainty (see Table 1 and 2).

For $N_2+N \rightarrow 2N+N$ reaction, the rate, again, was re-interpreted by Park[36] from three different sets of measurements. The recommended rate constants of Park have substantial uncertainty at lower temperatures (T ~10,000 K) because there are not enough N atoms to get a good fidelity measurement. We use slightly more than one order to magnitude ($4\sigma = 1.2$ in the $\log_{10}$ scale) uncertainty, as recommended by Park, for this reaction. The rates for N_2 dissociation by other atomic collision partners (C and H) are taken to be the same as the rate of $N_2+N \rightarrow 2N+N$. However, since H is a light atom, its effect on N_2 dissociation could be substantially different. To the best of our knowledge, the rates for N_2 dissociation upon atomic hydrogen impact do not exist in the literature. Therefore, we assume a larger uncertainty of one and one half orders of magnitude ($4\sigma = 1.5$ in the log10 scale).

The dissociation of the hydrocarbon molecules (CHx, x=1-4) is fast enough that most of the hydrocarbon molecules are rapidly converted into H and C atoms and some diatomics, such as CN, C_2 and NH via exchange reactions. Since the dissociation of CHx molecules is nearly complete [see Fig. 1(b)] the uncertainties in their rates are unlikely to be propagate through the system. In this work uncertainties are assigned to these reactions from the sources listed in Table 1. For CN dissociation the uncertainty is assigned from the compilations of Baulch *et al*.[22,24]

2. *Exchange Reactions*

The exchange reactions that we consider are also listed in Table 1. The rates and the uncertainties are taken from the listed references. CN, the primary radiating species, is produced mostly by the $N_2+C \rightarrow CN+N$ exchange reaction. The rate of this reaction in the reverse direction has been measured only up to 4000K. [22,24] We use the uncertainty recommended by Baulch *et al*. [22,24] Another reaction that is likely to be of importance is the $N_2+H \rightarrow NH+N$ exchange due to the abundance of N_2 and H in the shock layer. The rate of this reaction is also available only up to 4000 K.[22,24] Extrapolation of these reactions to typical shock layer temperatures of 10,000K will increase the rate uncertainty further, which is also considered. The remaining reaction rates and uncertainties are given in Table 1.

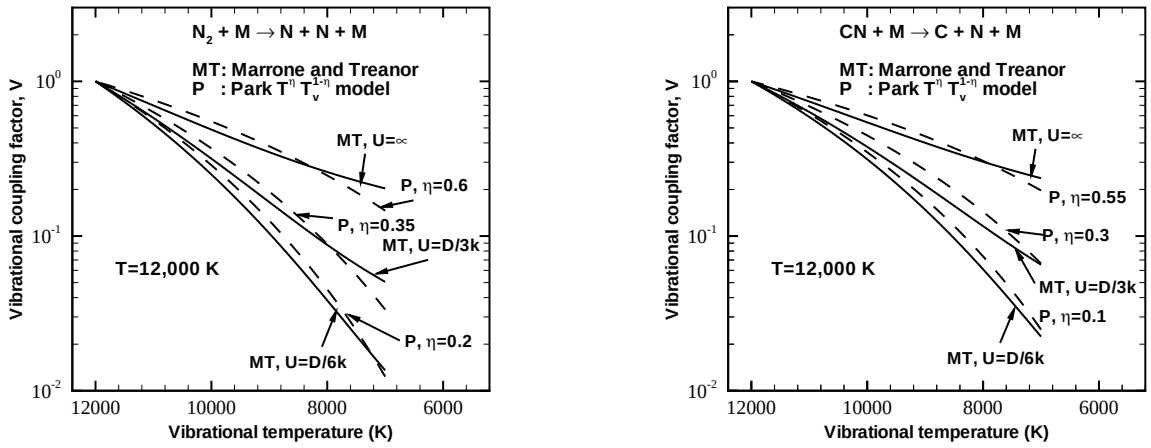

(a) (b)

Fig. 2. Vibrational coupling factors for (a) $N_2+M \rightarrow 2N+M$ and (b) $CN+M \rightarrow C+N+M$ reactions. It is shown that the variability of U in the Marrone and Treanor model is fairly well reproduced by varying the averaging weight η in the Park's $T^{\eta} T_v^{1-\eta}$ model.

B. Vibration-Chemistry Coupling:

The effect of vibrational nonequilibrium on the rates of chemical reactions is another source of uncertainty. It is well understood that a low vibrational temperature compared to the translational-rotational temperature slows

the rate of dissociation of molecules. Marrone and Treanor[37] formulated a preferential dissociation model based on the vibrational level of the dissociating molecule. This model describes the variable dissociation probability using an exponential term U as the characteristic parameter. $U=\infty$ represents the non-preferential limit (i.e. constant dissociation probability irrespective of the vibrational level) and $U=D/6k$ is the highly preferential dissociation probability case, where D is the dissociation energy of the diatomic. The uncertainty, therefore, lies mainly in the value of U, which defines the vibrational coupling factor, $V= k_r(T)/k_r(T,T_v)$, where $k_r(T)$ is the one temperature rate and $k_r(T,T_v)$ is thermal nonequilibrium rate. Later, Park introduced an empirical formula, $T_a = T^{\eta}T_v^{1-\eta}$, where a weighted geometric average of the temperatures can be used as an effective temperature to evaluate the rate constants when nonequilibrium is present.[36] Due to its simplicity and the ease of implementation in the code, Park's formula is used by most aerothermal codes, including DPLR. In this section, we estimate the uncertainty in the value of η by calibrating it against the variability in the value of U used in the Marrone and Treanor model. Marrone and Treanor[37] have shown that experimental data on N_2 and O_2 dissociation can be matched by $U=D/3k$ or $D/6k$, if the relaxation rates are adjusted accordingly. We assume that the uncertainty in vibration dissociation coupling can be incorporated by assuming an uncertainty in the value of U from infinity to $D/6k$. The equivalent uncertainty in Park's two temperature model can be roughly described by varying the averaging weight η. The variability in η is estimated by comparing with the vibrational coupling factor, V, obtained from the model of Marrone and Treanor, as shown in Fig. 2. These figures show the reduction in the rates of N_2 and CN dissociation as T_v is lowered while T is held constant at 12,000K. It is apparent that a variation of η from 0.1 to 0.6 describes the limits of uncertainty equivalent to the ones predicted by Marrone and Treanor model for the vibrational coupling factor V. We, therefore, assume a symmetric Gaussian bounded (with 95% probability) by these values with the most probable value of η=0.35 and 2σ=0.25. Although, Park's two temperature model is not based on rigorous physical analysis, the variation of η may adequately describe the uncertainty due to vibration dissociation coupling.

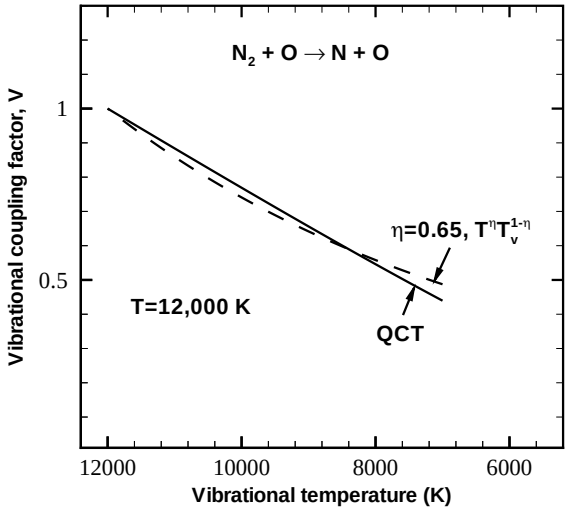

Fig. 3. The value of the averaging weight η in the Park's $T^{\eta}\ T_v^{1-\eta}$ model if applied to the exchange reaction is estimated from the quasi-classical trajectory data of N_2+O→NO+N reaction.

It is believed that rates of exchange reactions may also be affected by vibrational nonequilibrium. It is known that reaction probabilities of endothermic reactions of the type AB+C→AC+B are strongly dependent on the vibrational energy of AB. From a classical mechanics point of view, the reaction barrier for an endothermic reaction typically lies in the product (AC+B) channel of the potential energy surface, which is efficiently overcome by energy in the vibrational mode of AB. However, unlike vibration dissociation coupling there are no models or empirical formulas that are routinely used to express vibrational coupling with the exchange reactions. In this work we describe their uncertainty by assuming a Park $T^{\eta}T_v^{1-\eta}$ type effective temperature. Since there are no generally accepted values of η appropriate for exchange reactions, we use the quasiclassical trajectory data for the

N_2+O→NO+N reaction[38] to arrive at a reasonable estimate. Figure 3 shows the best value of η that describes the vibration coupling factor, V, deduced from the quasiclassical trajectory data at 12,000K. It is also reasonable to assume that the estimated value of η will vary somewhat with the translational-rotational temperature, and also from reaction to reaction. For the purposes of this paper we assume that the uncertainty in η from exchange reaction is same as the assumed uncertainty in its value for the dissociation reactions.

C. Vibrational Relaxation Time

The relaxation time between the vibrational and the translational mode is computed from the Millikan and White formula,[14]

$$\log\left(p\tau_{VT}\right) = A_{sr}(T^{-1/3} - 0.015\mu_{sr}^{1/4}) - 18.42$$
$$A_{sr} = 1.16\times10^{-3}\mu_{sr}^{1/2}\theta_{vs}^{4/3} \tag{3}$$

μ_{sr} and θ_{vs} are the reduced molecular weight of the species s and r and characteristic vibrational temperature of species s respectively and p is the pressure in atm. This formula fits a variety of vibrational relaxation data from independent measurements into a concise expression. It is shown that not only does log ($p\tau_{VT}$) vary in a straight line with $T^{-1/3}$, but also that these lines representing various collision pairs intersect at a single point, once a reduced mass correction is added. The uncertainty in τ_{VT} obtained from (3) may actually be lower than that in measurements because a universal fit across several sources of data, such as this, tends to eliminate random and systematic errors in measurements. However, for many of the binary interactions that occur in the Titan shock layer, this fit has not been verified due to a lack of experimental data. Nevertheless, we assume that this formula is valid for all interactions and only the slope of the log ($p\tau_{VT}$) versus $T^{-1/3}$ may be somewhat uncertain. We assign a ±6% uncertainty (95% confidence limits) to the slope of this line, which is sufficient to span the cloud of all sets of experimental data presented by Millikan and White.[14] A precise determination of this uncertainty is not necessary since, as will be shown later, τ_{VT} does not contribute significantly to the uncertainty in the radiative heating predictions.

D. Transport Properties

The methods used in the computation of mixture viscosity and thermal conductivity in DPLR have been shown to be in excellent agreement with more accurate Chapman-Enskog based representations in this flight regime[39,40] The SCEBD (self-consistent effective binary diffusion) model has similarly been shown to be an excellent approximation to more detailed multi-component representations.[41] All transport properties are based on collision integrals for each possible binary interaction in the flowfield, and thus the accuracy of the final quantities is dependent on the individual accuracies of each binary interaction quantity. The collision integrals used in this work come from a variety of sources and range widely in their assumed uncertainty, from less than 5% for interactions such as N-N and N_2-N, which have been determined through *ab initio* methods,[42,43] up to possibly 50% for trace interactions between radical species where no experimental or computational data are available. For this application uncertainty in transport properties is not expected to contribute significantly to the overall uncertainty, since most of the radiation occurs in the inviscid portion of the shock layer. Therefore we assign an arbitrary ±20% (95% confidence limit) uncertainty to the collision integrals of all binary interactions in this work. More care would be required in assigning uncertainties when convective heating is of primary interest.

V. Results and Discussion

A. Uncertainty in Radiative Heating Prediction

The next step in our Monte Carlo approach is to sample sets of input parameters based on Gaussian probability distributions representing the uncertainties assigned in the last section. In this work a total of 417 parameters (156 dissociation rate constants, 14 exchange reaction rate constants, 26 vibration coupling parameters, 130 vibrational-translational relaxation rates, and 91 transport properties) are independently selected in each set of input parameters. A total of 6000 such sets of input parameters are sampled to adequately describe their uncertainties. Figure 4 (a) shows the distribution of one of the reaction rate coefficients (N_2+H→2N+H), as represented by statistical sampling. The purpose here is to demonstrate that the input uncertainties are well represented by a sample size of 6000. The assigned uncertainty for this reaction is σ=0.375 (4σ=1.5 from Table II), whereas the standard deviation of the sampled set is about 0.38, which is sufficiently close to the assigned value for this rate constant.

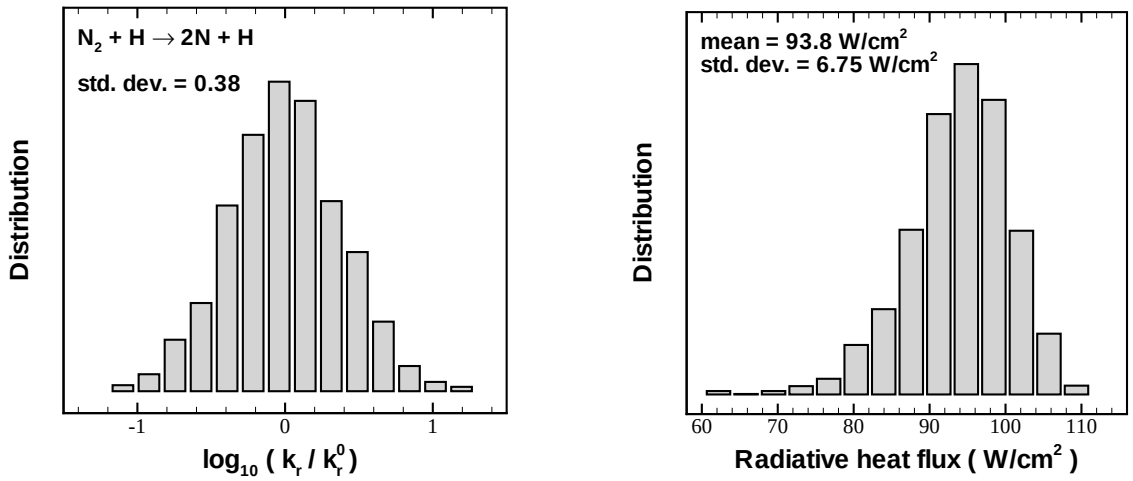

(a) (b)

Fig. 4. (a) Distribution of rate constants of N_2+H→NH+N reactions sampled using a Gaussian distribution function (sample size=6000). (b) Distribution of the stagnation point radiative heat flux, q_{rad}, obtained by collecting the output from DPLR.

Once the sets of input parameters are selected, a DPLR run is made for each set and the output variables of interest are collected. Since in this work we are interested only in the stagnation point radiative heating value, hereafter referred to as q_{rad}, an additional post processing step is necessary to compute this quantity from the flowfield data using the tangent slab approximation. Once the values of q_{rad} corresponding to all sets of input parameters are computed, they are binned to obtain a probability distribution representing the uncertainty in the stagnation point heat flux, as shown in Fig. 4(b). The 95% confidence limit is found to be between 81 W/cm^2 to 104 W/cm^2 with 93.8 W/cm^2 as the most probable value. This distribution is slightly asymmetric despite symmetric distributions of all input parameters due to uncertainty interference caused by non-linearities in the overall model (governing equations, chemical kinetics, etc.). Figure 4(b) is one of the key results of this work, which demonstrates that the combined effect of uncertainties in all of the input parameters considered in Table I and II cause about 24.3% overall uncertainty (95% confidence limits) in the stagnation point radiative heat flux, q_{rad}. This should be viewed as a lower estimate of the uncertainty in the prediction of q_{rad} since additional uncertainty will be caused by structural uncertainty in the model.

B. Input-Output Correlations

In a non-linear system, it is generally not possible to separate the contributions of each input parameter to the output uncertainty. Nevertheless, a linear regression analysis is often employed to roughly gauge the uncertainty contributions. In this section we will present correlation plots of q_{rad} versus some of the key input parameters. A square of the correlation coefficient, r_{ij}^2, can be interpreted as the fractional contribution to the uncertainty in the output y_j due to the uncertainty in the input parameter x_i. It must be emphasized here that since we use a finite sample size of 6000, there are statistical errors in the determinations of r_{ij}. We have made a manual estimate of the statistical error by varying the sample size and found that the error in the determinations of r_{ij}^2 is about ±0.02 (or ±2% contribution to q_{rad}). Therefore, the large contributions to q_{rad} uncertainty will be predicted with reasonable accuracy, while the small contributions will have significant errors. However, in practice, we only seek to identify and eliminate the small uncertainty contributors, not to evaluate their precise contributions.

Figure 5(a) and (b) show the correlation plots of q_{rad} with the rate constants of the N_2+H→2N+H and N_2+C→CN+N reactions respectively. Out of 429 input parameters considered, the rates of these reactions show some of the strongest influence on the value of q_{rad}, as shown by the relatively high correlation coefficients r_{ij}.

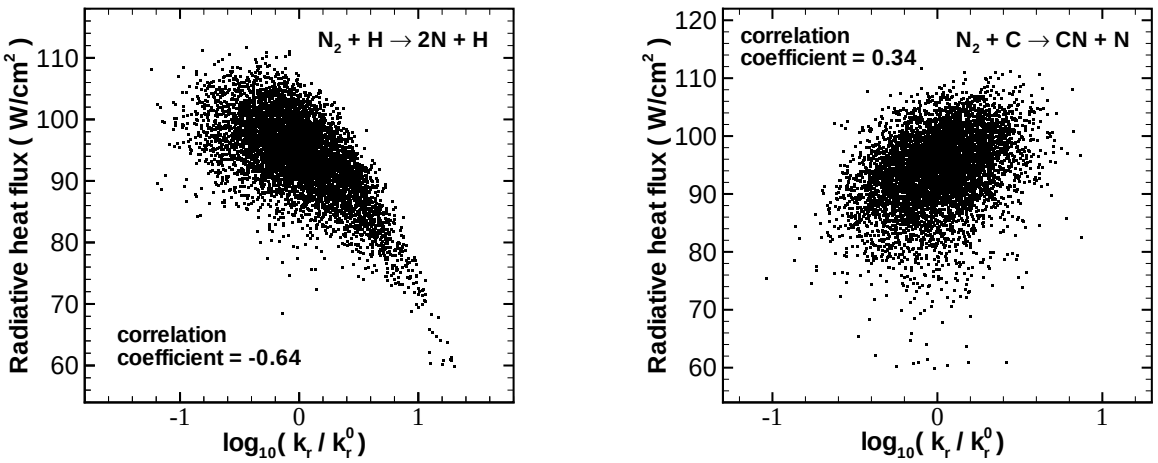

(a) (b)

Fig. 5. Correlation plots showing the influence of the rates of (a) N_2+H→2N+H and (b) N_2+C→CN+N reactions on the stagnation point radiative heat flux, q_{rad}.

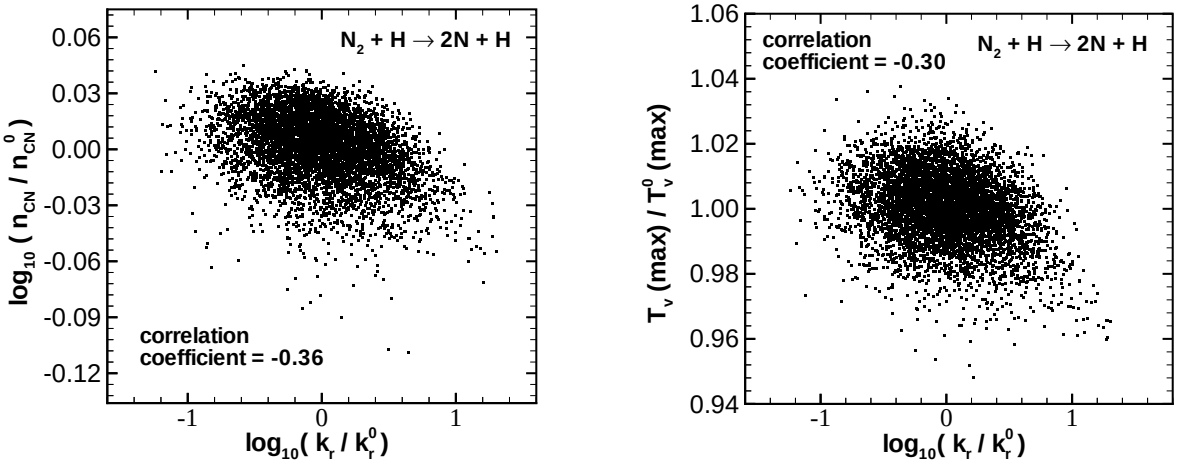

(a) (b)

Fig. 6. Correlation plots showing the influence of N_2+H→2N+H reaction on the (a) peak CN density and (b) peak vibrational temperature on the stagnation streamline (outside the boundary layer). The quantities with "0" as superscript represent the average values of the sample.

A strong influence of N_2+H→2N+H dissociation rate on the variability of the radiative heat flux is due to a combination of two factors. First, q_{rad} is found to be quite sensitive to the changes in the rate of this reaction. Second, the rate constant itself has a large uncertainty, as discussed earlier. This is analogous to right hand of equation (1) which shows, although strictly only for linear systems, that the uncertainty in the output $\sigma(y_i)$ is a combination of the sensitivity coefficient $\partial y_i/\partial x_k$ and the uncertainty $\sigma(x_k)$ in the input parameter. Although q_{rad} is more sensitive to the rates of other N_2 dissociation reactions such as N_2+N_2→2N+N_2, their contribution to the uncertainty in q_{rad} is smaller due to their smaller rate uncertainties (see Table I). The sensitivity to N_2 dissociation rates, in general, comes from the fact that this relatively highly endothermic process (heat of reaction = 9.8 eV) depletes some of the usable energy from the shock layer, which would have otherwise gone toward forming more CN molecules and exciting more of them to higher electronic states. Therefore, an increase in N_2 dissociation rate results in a smaller q_{rad} [see Fig. 5(a)]. The reduction in CN density with a rise in the dissociation rate is confirmed in Fig. 6(a), which shows a moderate negative correlation. This reduction can be attributed to a reduction in the shock layer temperatures which also show a negative correlation [see Fig. 6(b)]. A similar reduction in translational-

rotational temperature is also observed, but not plotted. The lower shock layer temperatures also cause less excitation of CN to higher electronic states, further reducing the CN radiation.

The exchange reaction N_2+C→CN+N also affects the CN radiation but to a lesser extent, as seen in Fig. 5(b). Since this reaction is responsible for formation of CN in the shock layer, where recombination is weak, an increase in its rate constant increases the CN density, and consequently the CN radiation. The affect is clearly seen in Fig. 7(a), which shows a large positive correlation coefficient of CN number density with the rate of this reaction. Its affect on the overall shock layer temperatures is, however, minimal as evident from Fig. 7(b).

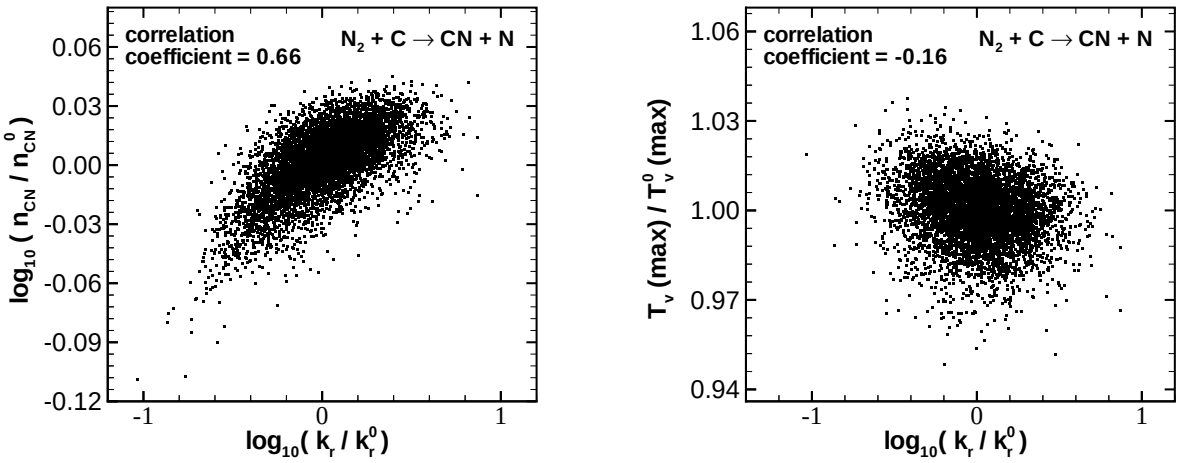

(a) (b)

Fig. 7. Correlation plots showing the influence of N_2+C→CN+N reaction on the (a) peak CN density and (b) peak vibrational temperature on the stagnation streamline (outside the boundary layer). The quantities with "0" as superscript represent the average values of the sample.

C. Uncertainty Ranking

As mentioned in the last section, using the square of the correlation coefficient, one can prioritize the input parameters according to their contributions to the uncertainty in q_{rad}. Figure 8(a) shows the eight largest contributors of uncertainty with their fractional contributions along the abscissa. The rate of dissociation of N_2 with H as the collision partner is found to be the largest source of uncertainty for the reasons discussed in the last section. The second largest contribution to the uncertainty is the N_2+H→NH+N reaction, which occurs readily because of abundance of N_2 and H in the shock layer (see Fig 1). Moreover this reaction is quite endothermic (6.1 eV), which acts to cool the shock layer resulting in less CN radiation. In addition to the high sensitivity, the rate of this reaction is quite uncertain at the shock layer temperatures (T~10,000 K) since experimental determination of the rate has only been done below 4000 K, as discussed earlier. The rate of the N_2+C→CN+N reaction, which is the primary pathway of CN formation, contributes only about 12% of the q_{rad} uncertainty. The effect of this reaction was discussed in the last section.

The remaining relatively large uncertainty contributors are the rates of various collision induced dissociation reactions. The rates of dissociation of the most abundant diatomic, N_2, with N and N_2 as collision partners, cause the largest sensitivities, but are only the 4th and 6th contributors of uncertainty. This is because these reactions have been better characterized by several shock tube measurements followed by a reinterpretation of the data. The dissociation of H_2, NH and CN may not significantly alter the shock layer temperatures, but instead they control the critical radical densities needed along the pathways of creation and consumption of CN. The dissociation of H_2 and NH produce H atoms, which enhance the influence of the influence of the first two reactions in Fig. 8(a). The dissociation of CN, obviously, depletes CN and thereby reducing radiation.

A complete representation of the uncertainty contributions is shown in Fig. 8(b). The rates of the dissociation reactions are responsible for the majority (64%) of the uncertainty, mostly because they largely determine the shock layer temperatures and their rates often have large uncertainties. The rates of the exchange

reactions are responsible for about 26% of the uncertainty in q_{rad}. The sensitivity due to these reactions is primarily because of the heat release or consumption and their role in CN formation pathways.

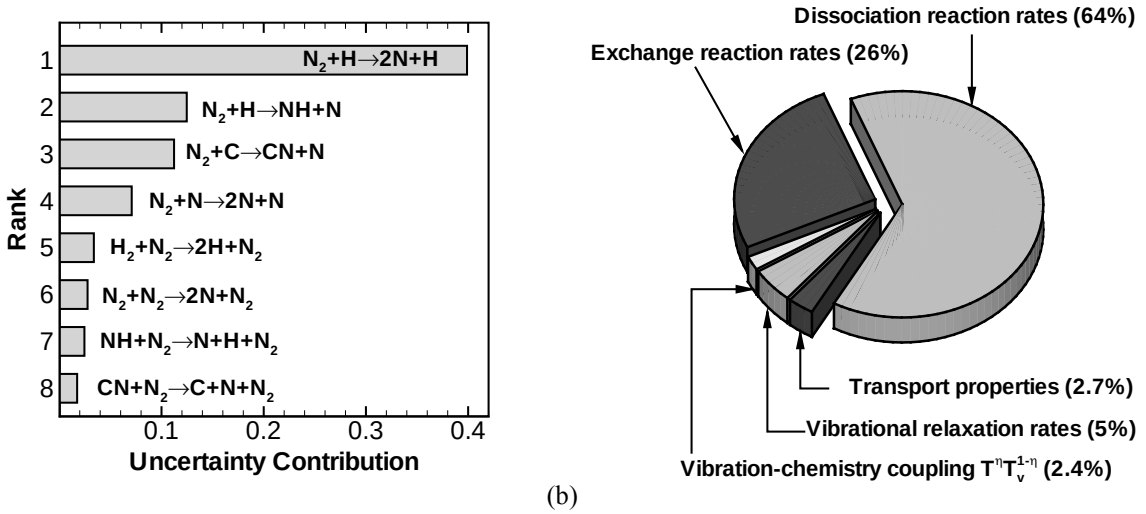

(a) (b)

Fig. 8. (a) The 8 largest contributors of uncertainty to q_{rad}, among all input parameters considered, are the rate constants of the reactions shown. The individual contributions to the uncertainty are plotted on the abscissa. (a) Percentage uncertainty contributions to q_{rad} from different categories of input parameters.

The vibrational-translational (VT) relaxation rate contributes to only a smaller portion (5%) of the uncertainty since the radiating portion of the shock layer is mostly in thermal equilibrium. The uncertainties in VT rates are therefore mostly suppressed, which also explains the small contribution (2.4%) of the uncertainty due to the vibration-chemistry coupling. The transport properties (viscosity, diffusion, and thermal conductivity), as expected, also contribute minimally to the uncertainty in the radiative heating value. The effect of transport properties are expected to be restricted within the cold boundary layer, which does not radiate appreciably. In other shock layers, where an optically thick boundary layer exists, the effect of uncertainties in the transport properties on q_{rad} would be higher.

VI. Concluding Remarks and Summary

A Monte Carlo technique for sensitivity and uncertainty analysis for non-linear systems with large input uncertainties is presented. The technique is applied to the aerothermal analysis of Titan aerocapture to rank the input parameters based on their contributions to the uncertainty in the predicted vehicle heating. First, the uncertainties in the input parameters are evaluated either from the literature or by reasonable estimates. Gaussian distribution functions representing these uncertainties are used to sample the input parameter. The results, although somewhat subjective, suggest that the largest sources of uncertainty lie in the lack of knowledge of the chemical reaction rates. The big contributors of the uncertainty are the rates of dissociation of N_2 by H atom impact and the two exchange reactions: $N_2+H\rightarrow NH+N$ and $N_2+C\rightarrow CN+N$. The dissociation of N_2, due to its large endothermicity, cools the shock layer, resulting in not only a low CN density, but also a lower level of electronic excitation of CN. However, the reason N_2 dissociation by H atom impact is the largest contributor is that the rate of this reaction itself is very uncertain compared to the N_2 dissociation with other important collision partners. The rate of exchange reaction $N_2+H\rightarrow NH+N$ is also a large contributor because of the same reasons. The $N_2+C\rightarrow CN+N$ reaction, however, is important because it controls the density of CN in the shock layer.

It is also found that the uncertainties in the vibrational relaxation times and vibrational-chemistry coupling parameters do not add much to the uncertainty in the radiation predictions mainly because the region of vibrational nonequilibrium in the shock layer is small. The transport properties also make only a small contribution because their effects are mostly restricted to the boundary layer, which does not radiate.

It must, however, be mentioned that the uncertainty ranking and the net parametric uncertainty in the radiative heat flux will likely vary, although not drastically, at different points in the entry trajectory. A comprehensive uncertainty analysis must involve analyzing many points along the trajectory and compute the uncertainty in the heat load. Also, the analysis presented here is mission specific and conclusions drawn here may not be valid if the mission specifications differ in terms of entry velocities, vehicle size, etc. Each candidate mission must, therefore, be analyzed individually to identify the pertinent uncertainties.

The results of such an analysis are useful during various phases of research, development and planning.

1) First and foremost, this analysis allows one to evaluate the uncertainty or confidence limits associated with the predictions of the aerothermal environment.
2) The analysis also identifies the target areas where the research effort should be directed to maximize payoff.
3) During experimental investigations, sensitivity analysis data are necessary to interpret the measurements and to possibly reduce uncertainties in the model parameters. The precision level needed in the experimental measurements aiming to reduce model parameter uncertainties can also be specified using the results of uncertainty analysis.
4) Such a probabilistic analysis, when all sources of uncertainty are included, can be integrated with probabilistic design[44] to determine more realistic design factors of safety corresponding to a desired level of TPS risk.

VII. Future Work

Although this article sheds light on the parametric uncertainties (reaction rates, vibration-chemistry coupling, relaxation times, and transport properties) associated with thermochemical models and their contributions to the Titan shock layer heating, additional sources of uncertainty due to structural uncertainties (inadequate formulations and simplifying assumptions) must also be addressed. In particular, we will explore the validity of the Boltzmann or the Quasi-Steady State (QSS) formulation for the determination of CN excited state populations included in the NEQAIR code. Since no reliable theoretical model currently exists, we will assess the impact of these uncertainties by comparing the predicted CN radiation with the shock tube measurements recently carried out at the Ames Research Center.

Acknowledgments

This work was funded by the In-Space Propulsion program under task agreement M-ISP-03-18 to NASA Ames. The work performed by Dr. Bose and Dr. Gökçen is supported by the prime contract NAS2-99092 to ELORET. We would also like to thank Dr. J. Olejniczak (NASA), Dr. D. Prabhu (ELORET), and Dr. David Hash (NASA) for useful discussions on reaction rates. The discussions with Dr. T.R. Govindan (NASA) on statistical sensitivity analysis are also acknowledged.

References

[1] Lockwood, M., "Titan Aerocapture Systems Analysis," AIAA Paper No. 2003-4799, Jul. 2003.

[2] Takashima, N, Hollis, B., Olejniczak, J., Wright, M., and Sutton, K., "Preliminary Aerothermodynamics of Titan Aerocapture Aeroshell," AIAA Paper No. 2003-4952, Jul. 2003.

[3] Olejniczak, J., Prabhu, D., Wright, M., Takashima, N., Hollis, B., Sutton, K., and Zoby, V., "An Analysis of the Radiative Heating for Aerocapture at Titan," AIAA Paper No. 2003-4953, Jul. 2003.

[4] Olejniczak, J., Bose, D., and Wright, M.J., "Aeroheating Analysis for the Afterbody of a Titan Probe," AIAA Paper No. 2004-0486, Jan. 2004.

[5] Wright, M.J., Bose, D., and Olejniczak, J., "The Impact of Flowfield-Radiation Coupling on Aeroheating for Titan," AIAA Paper No. 2004-0484, Jan. 2004.

[6] Wright, M.J., Loomis, M.A., and Papadopoulos, P.E., "Aerothermal Analysis of the Project Fire II Afterbody Flow," *Journal of Thermophysics and Heat Transfer*, Vol. 17, No. 2, 2003, pp. 240-249.

[7] Levin, D.A., R. J. Collins, G.V. Candler, M.J. Wright, and P.W. Erdman, "Examination of OH Ultraviolet Radiation from Shock-Heated Air," *Journal of Thermophysics and Heat Transfer*, Vol. 10, No. 2, pp. 200-208, Apr.-June 1996.

[8] Wright, M.J., R.J. Nowak, S.A. Berry, C.E. Glass, and G.V. Candler, "Numerical/Experimental Investigation of 3-D Swept Fin Shock Interactions," AIAA Paper No. 98-2816, June 1998.

[9] Olejniczak, J. and Fletcher, D.G., "An Experimental and Computational Study of the Freestream Conditions in an Arc-Jet Facility," AIAA Paper No. 2000-2567, Jun. 2000.

[10] Hollis, B.R. and Liechty, D.S., "Boundary Layer Transition Correlations and Aeroheating Predictions for Mars Smart Lander," AIAA Paper No. 2002-2745, June 2002.

[11] Wright, M.J., Prabhu, D.P., and Martinez, E., "Analysis of Afterbody Heating Rates on Apollo Command Modules, Part 1: AS-202," AIAA Paper No. 2004-2456, Jun. 2004.

[12] Wright, M.J., Candler, G.V., and Bose, D., "Data-Parallel Line Relaxation Method for the Navier-Stokes Equations," *AIAA Journal*, Vol. 36, No. 9, 1998, pp. 1603-1609.

[13] Gnoffo, P. A., "Computational Aerothermodynamics in Aeroassist Applications," AIAA Paper No. 2001-2632, 2001.

[14] Millikan, R.C. and White, D.R., "Systematics of Vibrational Relaxation," *Journal of Chemical Physics*, Vol. 39, No. 12, 1963, pp. 3209-3213.

[15] Gurvich, L., Veyts, I., and Alcock, C., eds., Thermodynamic Properties of Individual Substances, 4th Edition, Hemisphere Publishing Corporation, New York, 1991.

[16] Gokcen, T., "N2-CH4-Ar Chemical Kinetic Model for Simulations of Atmospheric Entry to Titan," AIAA Paper No. 2004-2469, June 2004.

[17] Gupta, R.N., Yos, J.M., Thompson, R.A., and Lee, K., "A Review of Reaction Rates and Thermodynamic and Transport Properties for an 11-Species Air Model for Chemical and Thermal Nonequilibrium Calculations to 30,000 K," NASA RP 1232, Aug. 1990.

[18] Park, C., Jaffe, R., and Partridge, H., "Chemical-Kinetic Parameters of Hyperbolic Earth Entry," *Journal of Thermophysics and Heat Transfer*, Vol. 15, No. 1, 2001, pp. 76-90.

[19] Ramshaw, J.D., "Self-Consistent Effective Binary Diffusion in Multicomponent Gas Mixtures," *Journal of Nonequilibrium Thermodynamics*, Vol. 15, No. 3, 1990, pp. 295-300.

[20] Whiting, E.E., Yen, L., Arnold, J.O., and Paterson, J.A., "NEQAIR96, Nonequilibrium and Equilibrium Radiative Transport and Spectra Program: User's Manual," NASA RP-1389, Dec. 1996.

[21] Saltelli, A., Chan, K., and Scott, E. M., *Sensitivity Analysis,* New York Wiley, 2001.

[22] Baulch, D. L., Cobos, C.J., Cox, R. A., Frank, P., Hayman, G., Just, Th., Kerr, J. A., Murrels, T., Pilling, M. J., Troe, J., Walker, R. W., and Warnatz, J., "Evaluated Kinetic Data for Combustion Modelling, Supplement I," *Journal of Physical Chemistry Reference Data*, Vol. 26, No. 6, 1994, pp. 847-1033.

[23] Dean, A. J., and Hanson, R. K., "CH and C-Atom Time Histories in Dilute Hydrocarbon Pyrolysis: Measurements and Kinetic Calculations," *International Journal of Chemical Kinetics*, Vol. 24, 1992, pp. 517-532.

[24] Kruse, T., and Roth, P., "Kinetics of C_2 Reactions during High-Temperature Pyrolysis of Acetylene," *Journal of Physical Chemistry A,* Vol. 101, 1997, pp.~2138-2146.

[25] Baulch, D. L., Cobos, C. J., Cox, R. A., Esser, C., Frank, P., Just, Th., Kerr, J. A., Pilling, M. J., Troe, J., Walker, R. W., and Warnatz, J., "Evaluated Kinetic Data for Combustion Modelling," *Journal of Physical Chemistry Reference Data*, Vol. 21, No. 3, 1992, pp. 411-429.

[26] Park, C., Howe, J.T., Jaffe, R.L., and Candler, G.V., "Review of Chemical-Kinetic Problems of Future NASA Missions, II: Mars Entries," *Journal of Thermophysics and Heat Transfer*, Vol. 8, No. 1, 1994, pp. 9-23.

[27] Tsang, W., "Chemical Kinetic Data Base for Propellant Combustion II: Reactions Involving CN, NCO, and HNCO," *Journal of Physical Chemistry Reference Data*, Vol. 21, No. 4, 1992, pp.~753-791

[28] NIST Chemical Kinetics Database, Version 7.0, 2003. (http://kinetics.nist.gov)

[29] Tsang, W., and Herron, J. T., "Chemical Kinetic Data Base for Propellant Combustion I. Reactions Involving NO, NO_2, HNO, HNO_2, HCN and N_2O," *Journal of Physical Chemistry Reference Data*, Vol. 20, No. 4, 1991, pp. 609-663.

[30] Dean, A. J., Hanson, R. K., and Bowman, C. T., "High Temperature Shock Tube Study of Reactions of CH and C-Atoms with N_2," *Twenty-Third Symposium (International) on Combustion/The Combustion Institute*, 1990, pp. 259-265.

[31] Sommer, T., Kruse, T., and Roth, P., "Perturbation Study on the Reaction of C_2 with N_2 in High-Temperature C_{60}/Ar + N_2 Mixtures," *Journal of Physical Chemistry A*, Vol. 101, 1997, pp. 3720-3725.

[32] Wooldridge, S. T., Hanson, R. K., and Bowman, C. T., "A Shock Tube Study of Reactions of CN with HCN, OH, and H_2 using CN and OH Laser Absorption," *International Journal of Chemical Kinetics*, Vol. 28, 1996, pp. 245-258.

[33] Davidson, D. F., and Hanson, R. K., "High Temperature Reaction Rate Coefficients Derived from N-Atom ARAS Measurements and Excimer Photolysis of NO," *International Journal of Chemical Kinetics,* Vol. 22, 1990, pp. 843-861.

[34] Dean, A. J., Davidson, D. F., and Hanson, R. K., "A Shock Tube Study of Reactions of C Atoms with H_2 and O_2 Using Excimer Photolysis of C_3O_2 and C Atom Atomic Resonance Absorption Spectroscopy," *Journal of Physical Chemistry*, Vol. 95, 1991, pp. 183-191.

[35] Nelson, H.F., Park, C., and Whiting, E.E., "Titan Atmospheric Composition by Hypervelocity Shock Layer Analysis," *Journal of Thermophysics and Heat Transfer*, Vol. 5, No. 2, 1991, pp. 157-165.

[36] Park, C., *Nonequilibrium Hypersonic Aerothermodynamics*, Wiley, New York, 1990.

[37] Marrone, P. V. and Treanor, C. V., "Chemical Relaxation with Preferential Dissociation from Excited Vibrational Levels," *Physics of Fluids*, Vol. 6, 1963, pp 1215-1221.

[38] Bose D. and Candler, G.V., "Detailed modeling of the Zeldovich reactions in hypersonic flows,'' *Journal of Thermophysics and Heat Transfer*, Vol. 12, No. 2., pp 214-222, Apr-Jun 1998.

[39] Palmer, G.E. and Wright, M.J., "A Comparison of Methods to Compute High Temperature Gas Viscosity," *Journal of Thermophysics and Heat Transfer*, Vol. 17, No. 2, 2003, pp. 232-239.

[40] Palmer, G.E. and Wright, M.J., "A Comparison of Methods to Compute High Temperature Gas Thermal Conductivity," AIAA Paper No. 2003-3913, Jun. 2003.

[41] Sutton, K. and Gnoffo, P.A., "Multi Component Diffusion with Application to Computational Aerothermodynamics," AIAA Paper No. 98-2575, June 1998.

[42] Levin, E. and Wright, M., "Collision Integrals for Ion-Neutral Interactions of Nitrogen and Oxygen," *Journal of Thermophysics and Heat Transfer*, Vol. 18, No. 1., pp 143-147, Jan-Mar 2004.

[43] Stallcop, J., Partridge, H., and Levin, E., "Effective Potential Energies and Transport Cross Sections for Atom Molecule Interactions of Nitrogen and Oxygen," *Physical Review A*, Vol. 64 (042722), 2001.

[44] Dec, J. A. and Mitcheltree, R. A., "Probabilistic Design of Mars Sample Return Earth Entry Vehicle Thermal Protection System," AIAA Paper No. 2001-0910, Jan 2001.